Dyes and Pigments 162 (2019) 494–511

Contents lists available at ScienceDirect

Dyes and Pigments

journal homepage: www.elsevier.com/locate/dyepig

Fibre optic reflectance spectroscopy and multispectral imaging for the non-invasive investigation of Asian colourants in Chinese textiles from Dunhuang (7th-10th century AD)

Diego Tamburini*, Joanne Dyer

Department of Scientific Research, The British Museum, Great Russell Street, London, WC1B 3DG, UK

ARTICLE INFO

Keywords:
Asian dyes
Multispectral imaging
FORS
Dunhuang
Silk road textiles

ABSTRACT

The archaeological complex of Dunhuang (northwestern Gansu, China) is considered a pearl on the Silk Road and the content of its caves revolutionised oriental studies. The British Museum hosts a significant number of textiles and textile fragments from the site. Although mostly catalogued and studied from the point of view of textile production, weaving techniques and iconography, they have never undergone dye analysis, which is here presented for the first time. Due to the value, preciousness and fragility of these textiles, sampling is not always an option. Therefore, a non-invasive approach combining multispectral imaging (MSI) and fibre optic reflectance spectroscopy (FORS) was tested. The final aims of this research were to explore the advantages and limitations of such an approach with application to Asian dyes and ultimately to provide new insights into the technological skills related to dyestuff production and use in ancient China.

To achieve these aims, twenty-nine reference specimens of Asian dyes were sourced, including sappanwood (*Biancaea sappan*), sandalwood (*Pterocarpus santalinus*), different species of madder (*Rubia* spp.), rosewood (*Dalbergia* sp.), rhubarb (*Rheum emodi*), dragon's blood (*Daemonorops* sp.), Indian lac (*Kerria lacca*), gromwell (*Lithospermum erythrorhyzon*), safflower (*Carthamus tinctorius*), amur-cork tree (*Phellodendron amurense*), gamboge (*Garcinia hanburyi*), violet (*Viola yedoensis*), pagoda tree (*Sophora japonica*). Silk was dyed using these raw materials and the reference samples were analysed by colorimetry before and after ageing. These measurements highlighted the most light-sensitive dyes to be turmeric, safflower, sappanwood and sandalwood. The reference samples were also used to create a database of reflectance and apparent absorption spectra obtained by FORS, as well as to record the reflectance, luminescence and absorption properties of specific dyes by MSI. The combined information obtained from MSI and FORS brought to the fore the signature behaviour of certain dyes (protoberberine-based dyes, safflower, gromwell, tannins, madder, sappanwood, Indian lac and indigo), which enabled their unequivocal identification and the mapping of their distribution in thirty-one Dunhuang textiles from the British Museum's collection.

The data presented in this work will be beneficial to other researchers and conservators investigating textiles from the Silk Road using a non-invasive approach and for the assessment of textiles and their suitability for display.

1. Introduction

The archaeological complex of Dunhuang in northwestern China is one of the most important sites of the Silk Road and the content of the so-called Hidden Library (Cave 17) revolutionised oriental studies. Sealed from the beginning of the 11th century, the cave contained documents, mural and silk paintings and textiles spanning the 6th to the 11th century [1]. These attracted the interest of scholars and archaeologists from around the world. Among them was Sir Aurel Stein, who acquired many objects and brought them to the UK in the early 1900s [2]. However, most of the attention was focused on the outstanding mural paintings and the materials used to create them, in order to attend to their preservation needs [3–7]. The textiles, which initially received less attention, consisted of canopies, banners, sutra covers and wrappers, polychrome and monochrome woven silk, clamp-resist dyed silk and embroidered silk [1]. Although these have been studied from a technological, stylistic and iconographic point of view, dye analysis is rare or rarely published regarding the Dunhuang textiles [8]. One of the

* Corresponding author. Department of Scientific Research, The British Museum, Great Russell Street, WC1B 3DG, London, United Kingdom.
E-mail address: DTamburini@britishmuseum.org (D. Tamburini).

https://doi.org/10.1016/j.dyepig.2018.10.054
Received 7 September 2018; Received in revised form 19 October 2018; Accepted 25 October 2018
Available online 26 October 2018
0143-7208/

aims of this work was therefore to analyse a significant number of Dunhuang textiles, dated from the 7th to the 10th century AD, in order to fill this gap in the current literature.

The identification of natural dyes is generally based on the comparison of the results obtained on an object with those obtained on reference samples. As people from different geographical locations have used natural dyes relying on the availability of their natural sources [9], the investigation of these materials in objects from specific geographical areas requires a high degree of knowledge of historically relevant and significant dye sources, as well as access to the appropriate reference materials. Sources of dyes used in the Tang dynasty (7^{th}-9th century) [10] and later periods [11] have been presented in the literature, as well as dye analysis on textiles from other important Asian archaeological sites [8,12–27]. This research has shed light on the most common sources of dyes used in Asia [10,11,14,16,28], but unidentified colourants are often reported in the literature addressing this topic [8,16–18,23,24], pointing towards the need for further research.

From the outset, this work aimed to create a set of reference samples of Asian dyes and utilise the data obtained as a robust base for the identification of natural dyes in Dunhuang textiles. Furthermore, two additional important aspects were carefully considered. Firstly, the importance of ageing and fading of natural dyes in making the presence of these in textiles visually unrecognisable is a well-known topic [29–32], but only a few studies are specifically available on Asian dyes [33,34]. Molecular degradation mechanisms have generally been studied [35–38] and, when these occur, the identification of certain types of dyes can be problematic. For these reasons, all the reference samples considered in this work were investigated before and after artificial ageing. Natural ageing is very difficult to simulate, as the history of a textile is generally difficult to be tracked down completely. However, although nothing can be done about the damage resulting from the natural ageing of a textile, risks related to further display can be avoided by knowing the light-sensitivity of the dyes. Display conditions in museums, however, can be simulated and accelerated and this was addressed in this paper. A further concern when dealing with dye analysis in textiles is the analytical approach employed [39]. It has been shown that high pressure liquid chromatography (HPLC) has the most potential in terms of the level of detail that can be obtained from this analysis [40–42] and this has been successfully applied for the identification of Asian dyes [8,12–24]. However, although the amount of sample required for HPLC-MS analysis is very small (2–3 mm of a single thread, *ca.* 100 μg) and the damage to knowledge-obtained ratio is very positive, sampling is not always possible when dealing with precious and fragile textiles and non-invasive approaches are highly desirable. Non-destructive or nano-destructive surface techniques, such as TOF-SIMS, SERS, FTIR, fluorescence and UV–Vis reflectance spectroscopies have been applied to identify a limited number of Asian colourants [16,25,43–45]. In particular, fluorescence and diffuse reflectance spectroscopies applied to Japanese woodblock prints have recently shown promise in this field, revealing some, albeit limited, information [46,47]. The main issue with the non-invasive investigation of dyes is related to the identification of yellow dyes, some of which are hardly distinguishable from each other in terms of their fluorescence and diffuse reflectance spectra [48].

Here, the integration of fibre optic reflectance spectroscopy (FORS) and multispectral imaging (MSI) is further explored in order to understand the full potential of these techniques applied to the identification of Asian dyes. FORS is well-known to be a rapid and effective non-invasive method, which has been applied to painted surfaces and textiles [49–52]. Measurements are very fast (less than 1 min per acquisition) and yield information on both reflectance and apparent absorption features. Similarly, MSI is well-established in the study of paintings and polychrome surfaces [53–56] and has recently seen its first systematic application to the investigation of Late Antique textiles [57], proving to be a powerful tool for the study of textiles and dye identification. This approach is extremely visual, thus providing information that can be easily accessible to conservators or other non-specialists. However, the acquisition and processing of the images must be conducted following rigorous and scientific protocols, in order to obtain comparable results [58]. The correct interpretation of MSI and FORS data has proved to be an extremely useful tool both in obtaining information on dye sources and in planning strategic sampling campaigns [57].

This approach (FORS and MSI), integrated with digital microscopy and colorimetric measurements, was here further challenged by being applied to a set of reference samples of Asian dyes and to thirty-one textiles from Dunhuang present in the collection of the British Museum, with the aim to create guidelines for the correct interpretation of MSI images and FORS data of Asian dyes. The set of reference samples created as a result of this research and the data obtained from their subsequent analysis are finally interpreted against the wider context of dye analysis of Asian textiles.

2. Materials and methods

2.1. Reference materials

Twenty-eight specimens of plant material and one specimen of sticklac from *Kerria lacca* (Indian lac dye) were collected from different sources, on the basis of available literature on natural sources of Asian dyes [9–11,16–18,33,45]. Because of the difficulties related to accessing some of these types of plants, different sources were used. *Phyllanthus emblica* (Indian gooseberry), *Rhus* spp. (Chinese sumac), *Rubia cordifolia* (Indian madder, munjeet), *Rubia tinctorum* (dyer's madder), *Rheum emodi* (rhubarb), *Dalbergia* sp. (rosewood), *Curcuma longa* (turmeric), *Gardenia jasminoides* (cape jasmine), *Symplocos* sp. (Lodh tree/Asiatic sweetleaf), *Viola yedoensis* (violet), *Phellodendron amurense* (amur-cork tree), *Garcinia hanburyi* (gamboge), *Crocus sativus* (saffron), *Reseda luteola* (weld) and *Kerria lacca* (Indian lac dye) were available from the British Museum reference collection. Another madder sample, referred to as “madder Thimpu” with no further descriptive details apart from the location of collection (Thimpu, Bhutan) was also available and used for comparison. According to the records, these materials were collected in 2006 and have been stored in the dark since then but no further information was available.

Rubia akane (Japanese madder), *Biancaea sappan* (sappanwood), *Lithospermum erythrorhizon* (gromwell), *Pterocarpus santalinus* (sandalwood), *Daemonorops* sp. (dragon's blood), *Sophora japonica* (pagoda bud) and *Coptis chinensis* (Chinese goldthread) were acquired at the Institute of Chinese Medicine (London, UK). These materials are imported from China on a regular basis and stored in the dark, but the exact collection time is not available.

Rhamnus saxatilis (buckthorn) was purchased from Kremer Pigmente in 2015 and has been stored in the dark since then. *Juglans regia* (walnut tree) husks were provided fresh by Mrs. Barbara Wills (Department of Conservation, British Museum) and used after a few days of fermentation.

Two samples of wool dyed with yellow and pink extracts of *Carthamus tinctorius* (safflower) were available. These were prepared for a separate set of experiments in 2014 from safflower petals collected in the same year. They had been stored in the dark since 2014 and then used as they were. Samples of silk dyed with extracts of *Miscanthus sinensis* (silver grass), *Cotinus coggygria* (smoke tree) and *Berberis thunbergii* (Japanese barberry) were provided by the Getty Conservation Institute (Los Angeles, USA). These were dyed in 2004 [10] and stored in the dark since then.

Apart from this last set of five pre-dyed samples, the rest of the plant (insect) material was used to create a set of reference dyed samples. Strips of silk[1] (*ca.* 0.6 g; 20 cm × 3 cm) were dyed with each dyestuff.

[1] Wool was also dyed with the original intention to have a systematic

Table 1
Brief description of the textiles analysed. The monochrome textiles are listed according to their colour.

Object number	Brief Description
Monochrome woven silk	
MAS.890	Yellow twill damask (it is described as orange). Stein noticed the polished surface of the fragments, which he believed was the result of heavy calendaring. Late 9th-early 10th century. Length 6 cm; width 11 cm
MAS.935	Yellow twill damask. Late 9th-early 10th century. Length 14 cm; width 2.5 cm
MAS.936	Bright yellow twill damask. It is described as orange. Late 9th-early 10th century. Length 10 cm; width 7.3 cm
MAS.938	Yellow lozenge twill damask. Late 9th-early 10th century. Length 5.8 cm; width 18.5 cm
MAS.942	Pale yellow damask on plain weave. Late 9th-early 10th century. Length 16.5 cm; width 15.5 cm
MAS.904	Orange patterned complex gauze. 7th-10th century. Length 9.7 cm; width 10.3 cm
MAS.951	Orange ribbed weave. It is described as bright red. Late 9th-early 10th century. Length 26.3 cm; width 3.4 cm
MAS.939	Red twill damask with floral patterns. Late 9th-early 10th century. Length 8.5 cm; width 8 cm
MAS.954	Red patterned complex gauze. Probably part of a layered streamer on a valance. 7th-10th century. Length 9.2 cm; width 10.3 cm
MAS.896	Damask on plain weave. Late 9th-early 10th century. It was probably purple now turned into brown. Length 15.5 cm; width 10 cm
MAS.949	Damask on plain weave. Late 8th-early 9th century. It looks brown but it was probably a different colour. Length 31.5 cm; width 8.5 cm
MAS.891	Purple twill damask. Late 9th-early 10th century. Same pattern as MAS.937. Length 9 cm; width 5 cm
MAS.900	Purple simple gauze with floats. Late 9th-early 10th century. Length 4.5 cm; width 8.3 cm
MAS.901	Purple simple gauze with floats. Late 9th-early 10th century. Length 22.5 cm; width 5.7 cm
MAS.902	Purple simple gauze with floats. Late 9th-early 10th century. Length 17 cm; width 3.8 cm
MAS.903	Purple simple gauze with floats. Late 9th-early 10th century. Length 6.5 cm; width 21 cm
MAS.937	Purple twill damask Late 9th-early 10th century. Same pattern as MAS.891. Length 14.5 cm; width 1.8 cm
Polychrome woven silk	
MAS.865	Part of 57 fragments originally forming a floral medallion on a red ground. Late 8th- early 9th century. Sogdian samite. Yellow, orange and blue colours. Length 4 cm; width 16.3 cm
MAS.869	Fragment with roundel pattern representing a phoenix. Late 9th-early 10th century. Liao samite. Purple, yellow, green and orange colours. Length 8 cm; width 3.2 cm
MAS.871	Floral medallion on red ground. Brocade on twill. 10th century Purple, red, yellow, pink and green colours. Length 2.7 cm; width 7.3 cm
MAS.872	Triangular fragment with Z-shaped and lozenge designs. Late 8th- early 9th century. Sogdian samite. Red, yellow, green and blue colours. Length 4 cm; width 4.1 cm
MAS.873	Narrow strip probably with floral roundels. Late 8th- early 9th century. Sogdian samite. Yellow, green, orange, red and blue colours. Length 19.3 cm; width 0.8 cm
MAS.906.a-b	Two narrow strips of silk tapestry (kesi) with floral pattern, perhaps showing part of a medallion. Probably part of a sutra wrapper. Late 7th – early 8th century. Yellow, orange, pink, purple, green, blue, brown colours. a: length 16.6 cm; width 1.4 cm - b: length 9.4 cm; width 1.3 cm
MAS.908.a-b	Two narrow strips of silk tapestry (kesi) with floral pattern on pink (red) background. Late 7th – early 8th century. Yellow, brown, pink, green and blue colours. a: length 7.5 cm; width 1.7 cm - b: length 8 cm; width 1.8 cm
MAS.920	Fragments representing geese, circles and quatrefoils. Late 9th-early 10th century. Liao samite. Pink, yellow and blue colours. Length 15.5 cm; width 6 cm
MAS.922	Heart-shaped petal design in red on a yellow ground. Late 8th- early 9th century. Sogdian samite. Yellow, red, orange and blue colours. Length 12.5 cm; width 4.5 cm
MAS.924	Fragment with stripes and flower motif. Double weave in silk. Late 7th early 8th century. Yellow, green and blue colours. Length 22.5 cm; width 5.5 cm
MAS.929	Fragment of a black ground with unrecognisable yellow (gold) decoration. Brocade on twill Late 9th-early 10th century. Black and yellow colours. Length 13.5 cm; width 7 cm
Embroidered silk	
MAS.911	Multi-coloured embroidery of a Buddha standing on a lotus pedestal and enclosed within an almond-shaped aureole. The ground is a plain woven dark brown silk and the embroidery is made with split and couching stitches. Late 8th- early 9th century. Brown, orange, green and blue colours. Length 10.9 cm; width 6.2 cm
MAS.915	Triangular black twill damask with a diamond pattern embroidered in satin stitch with motifs of half-florets. Late 9th-early 10th century. Pink, red, green and blue colours. Length 14 cm; width 6.3 cm
MAS.1130	Rectangular fragment of damask on plain weave in a faded red colour embroidered with split stitches to create a motif probably representing a peacock. Late 8th-early 9th century. Red, brown, yellow, pink, green, blue and purple colours. Length 21 cm; width 9 cm

Different parts of the plants (petals, fruits, roots, rhizomes, heartwood, *etc*.) were used according to traditional recipes [14,19,59]. The dyeing procedure was generally performed in two steps: the extraction of the dyes from the raw materials to create the dye baths and the actual dyeing of the fibres by soaking the silk in the dye bath, prior mordanting, if necessary.

Both alum- and iron-mordanted fabrics were dyed with dyer's madder. This was done to evaluate possible differences in the final chemical composition when different mordants are used [59]. With a similar aim, walnut extracts were used to dye both non-mordanted and alum-mordanted fabrics. Dyeing with sappanwood and sandalwood extracts was performed at both neutral and basic pH (addition of Na_2CO_3). It is reported that significant changes in colour can be obtained by changing the pH, especially for sappanwood [59].

The experiments described produced a set of twenty-nine silk reference samples to be added to the five samples already available. Undyed, alum-mordanted and iron-mordanted silk strips were used for comparison. The set of reference samples is shown in Figs. 4 and 5. A list of these samples and additional details of their production are included in a paragraph and in Table S1 in the Supplementary Information.

2.2. Archaeological textiles

Thirty-one textiles from the Stein collection of the British Museum were investigated in this project (seventeen monochrome woven silk, eleven polychrome woven silk and three embroidered silk textiles). The textiles, mainly fragments, are dated from the late 7th to the early 10th century (Tang to Five Dynasties period) and are representative of various weaving techniques (damask, gauze, brocade, samite, *etc*.). A brief description of these textiles is presented in Table 1 and images of most of them are shown in Figs. 1 and 7 and 9–11. These textiles have

(*footnote continued*)
comparison between the two sets of samples. The main difference observed was in the colour obtained after dyeing with specific dyes. Generally, most direct dyes gave a brighter colour on silk and most mordant dyes gave a brighter colour on wool. Apart from this difference, the colour changes obtained after artificial ageing and the results obtained by FORS and MSI were very similar. For this reason and, most relevantly, because all the investigated textiles were made of silk, the results obtained for the wool samples were not included. Nevertheless, most of the collected data are also valid for dyed wool.

Fig. 1. Top: images of some of the textiles under investigation Bottom: images obtained by digital microscopy showing the variety of weaving techniques: a) MAS.935 twill damask, b) MAS.942 damask on plain weave, c) MAS.954 patterned complex gauze, d) MAS.951 ribbed weave, e) MAS.891 twill damask, f) MAS. 904 patterned complex gauze, g) MAS.934 twill damask, h) MAS.896 damask on plain weave, i) MAS.949 damask on plain weave, j) MAS.900 simple gauze, k) MAS.872 sogdian samite, l) MAS.920 liao samite, m) MAS.871 brocade on twill, n) MAS.906 kesi, o) MAS. 924 double weave.

previously been technically and stylistically studied [1] and some digital microscopy images exemplifying the weaving techniques employed are presented in Fig. 1. The textiles show a wide range of colours in various shades, including brown, yellow, orange, pink, red, purple, green and blue.

2.3. Artificial ageing

Accelerated artificial ageing was performed on the set of reference samples to simulate the results of long-time exposure in a museum environment. Small squares of fabric (3 cm × 3 cm) or 2.5 cm threads in the case of safflower, silver grass, Japanese barberry and smoketree samples were sewn onto acid-free card using a barely visible cotton thread and put into an Atlas SolarClimatic SC 340 MH climatic chamber equipped with a metal halide lamp simulating solar radiation. A UV filter (5 mm LEXAN filter with a Sun-X MT20 film) was used to cut the radiation below 400 nm and reduce the total illuminance to 0.027 Mlux. Temperature (T) was set at 40 °C (higher then room temperature to accelerate the ageing) and relative humidity (RH) was set to 50%. The experiment lasted four weeks (672 h). As the visible light intensity

Table 2
Multispectral imaging and FORS apparent absorption features of the reference dye samples.

	VIS	UVL	IRRFC	UVRFC	FORS (nm)
Non-mordanted silk	White	Bluish (from silk)	White	Yellow	Featureless
Alum-mordanted silk	White	Bluish (from silk)	White	Yellow	Featureless
Iron-mordanted silk	Light brown	Black	Beige	Brown	Featureless
Indian gooseberry	Light brown	Black	Orange	Brown	Broad absorption
Walnut	Light brown	Black	Orange	Brown	Broad absorption
Chinese sumac	Dark brown	Black	Red	Brown	Broad absorption
Japanese madder	Orange	Pink/Orange	Yellow	Brown	430, 510, 540
Indian madder	Orange/red	Pink/Orange	Yellow	Brown	430, 510, 540
Dyer's madder	Orange/red	Pink/Orange	Yellow	Brown	Not structured
Dyer's madder + iron	Brownish red	Black	Orange	Brown	Not structured
Sappanwood	Red	orange (very weak)	Yellow	Green	540
Sappanwood + potash	Bright pink	Purplish (very weak)	Yellow	Green	560
Indian lac	Pink	Light pink (very weak)	Light yellow	Green	525, 560
Safflower pink	Pink	Bright orange	Yellow	Brown	515
Sandalwood	Red	Brick red	Yellow	Brown	480, 510
Sandalwood + potash	Red	Purplish (from silk)	Yellow	Brown	480, 510
Rosewood	Orange	Brown	Yellow	Brown	490, 600
Dragon's blood	Orange	Brown/yellow	Yellow	Brown	Not structured
Rhubarb	Yellow/orange	Dark	Beige	Orange	445
Gromwell	Purple	Bluish (from silk)	Pink	Green	510, 550, 595
Chinese goldthread	Deep yellow	Olive	Beige	Red	465
Japanese barberry	Bright yellow	Yellow	Beige	Red	445
Amur-cork tree	Bright yellow	Bright yellow	White	Orange	440
Turmeric	Deep yellow	Yellow-green	Lemon yellow	Red	460
Saffron	Yellow	Olive	Lemon yellow	Pink	445, 470
Cape jasmine	Yellow	Olive	Lemon yellow	Pink	445, 470
Safflower yellow	Yellow	Yellow (weak)	Lemon yellow	Red	440
Smoketree	Yellow	Yellow (weak)	White	Orange	430
Pagoda tree	Yellow	Olive	White	Orange	430
Gamboge	Yellow	Black	White	Yellow	420
Symplocos	Brownish yellow	Green	Beige	Yellow	420
Violet	Pale yellow	Bluish (silk)	White	Yellow	400
Silver grass	Brownish yellow	Bluish (silk)	White	Yellow	420
Weld	Yellow	Yellow-green	White	Orange	430
Buckthorn	Greenish yellow	Olive	White	Orange	420

is not completely homogeneous in the chamber, the card was rotated by 90° every week. All the samples were therefore exposed to *ca.* 18.15 Mlux during ageing.

2.4. Colorimetry

Colorimetric measurements of the reference samples were taken in triplicate (three different spots on the piece of fabric) before and after ageing using a Konika Minolta CM-2600d spectrophotometer equipped with a 52 mm barium sulphate integrating sphere, dual-beam geometry, di:8°, de:8°, a 360–740 nm wavelength range with 10 nm measurement intervals. The measuring area was 3 mm diameter and the standard illuminant was D65. A plate of barium sulphate was used as white reference to calibrate reflectance spectra. The CIE L*a*b* colour space was adopted. In this system L* represents the lightness (from 0 black to 100 pure white), a* is related to the red and green components (positive red – negative green) and b* is related to the blue and yellow components (positive yellow – negative blue). The data were recorded including the specular component, as the surface of the samples was not glossy. The data were then used to calculate the ΔE (2000) as the square root of $(\Delta L^*)^2 + (\Delta a^*)^2 + (\Delta b^*)^2$. This parameter is indicative of the total colour difference before and after ageing.

2.5. Digital microscopy (DM)

Digital microscopy was used to investigate the weaving of the textiles with the aim to highlight colour nuances, possible mixtures of dyes and fading. A Keyence VHX-5000 digital microscope was used to record magnified images (20-200x), equipped with a lens VH-Z 20R, an automated stage VHX-S 550E and LED reflected illumination.

2.6. Multispectral imaging (MSI)

The reference samples and the textiles were arranged on a black card together with a reference grey scale, comprising a set of Lambertian black, grey and white tiles (Spectralon®) and an XRite ColorChecker target. Images were taken using a modified Nikon D7000 camera body after removal of the inbuilt UV-IR blocking filter, in order to exploit the full sensitivity of the CMOS sensor (*ca.* 300–1000 nm). The camera was operated in fully manual mode.

The set of images acquired included visible-reflected (VIS), infrared-reflected (IRR), ultraviolet-induced visible luminescence (UVL), ultraviolet-reflected imaging (UVR), visible-induced visible luminescence (VIVL) and multiband-reflected (MBR) images. Infrared-reflected false colour (IRRFC) and ultraviolet-reflected false colour (UVRFC) images were produced combining VIS and IRR or UVR images respectively, as described in [58].

Generally, the object is illuminated by two radiation sources symmetrically positioned at approximately 45° with respect to the focal axis of the camera and at about the same height. A filter, or combination of filters, is placed in front of the camera lens in order to select the wavelength range of interest. The combinations of radiation sources and filter(s) used for each MSI technique are summarised in Table 2S (Supplementary Information). The entire process of acquiring the images lasted for approximately 1 h, of which 15 min were dedicated to UVL and UVR imaging. The risk of damage when exposing the textiles to a UV source for such a short amount of time can be considered negligible. Details about acquisition and post-processing of the images are reported in a previous publication [57].

The reference samples were imaged before and after artificial ageing. Both the front and the back of the archaeological textiles were imaged, as some weaving techniques produce different patterns on each

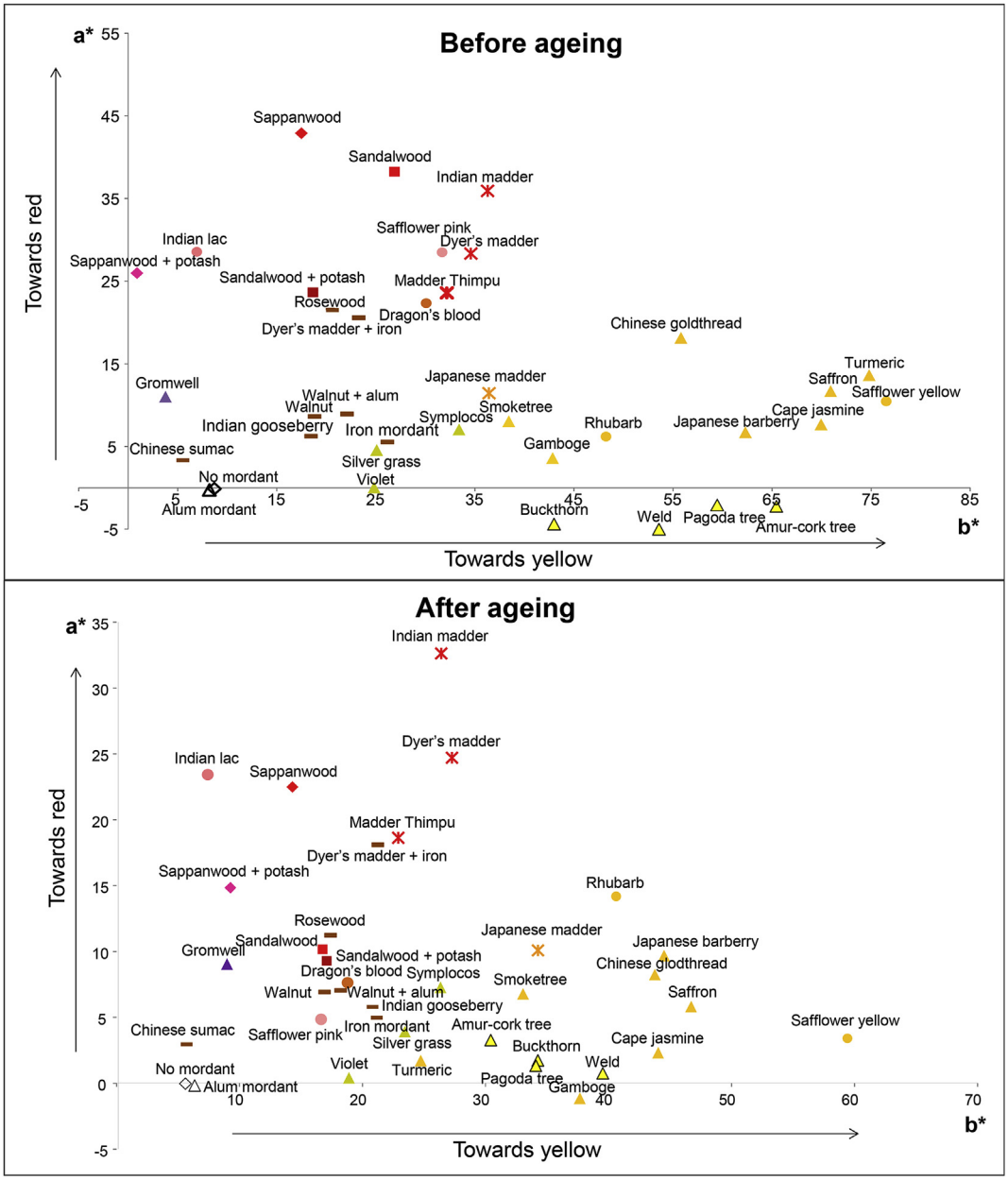

Fig. 2. Colour parameters obtained before and after artificial ageing of the reference samples projected on the a*b* plane of the CIE L*a*b* colour space. (For interpretation of the references to colour in this figure legend, the reader is referred to the Web version of this article.)

side. In addition, the effects of fading are often more notable on one side of the textile due to preferential display.

2.7. FORS

Fibre optic reflectance spectra were recorded for all the reference samples and all the coloured areas of the textiles with an Avantes (Apeldoorn, The Netherlands) AvaSpec-ULS2048XL-USB2 spectrophotometer equipped with an AvaLight-HAL-S-IND tungsten halogen light source. The detector and light source were connected with a fibre optic bundle to an FCR-7UV200-2-1.5 × 100 probe. In this configuration, light was sent and retrieved by the bundle set at approximately 45° from the surface normal, thus excluding specular reflectance. The spectral range of the detector was 200–1160 nm; nevertheless, due to poor blank correction on both the extremes of the range, only the range between 300 and 900 nm was considered; as per the features of the monochromator (slit width 50 μm, grating of UA type with 300 lines/mm) and of the detector (2048 pixels), the best spectra resolution was 2.4 nm calculated as full width at half maximum (FWHM). Spectra were referenced against the WS-2 reference tile provided by Avantes. The diameter of the investigated area on the sample was approximately 1 mm, obtained by setting the distance between probe and sample at 1 mm. The instrumental parameters were as follows: 50 ms integration time, 20 scans for a total acquisition time of 1 s for each spectrum. The whole system was managed by the software AvaSoft 8 for Windows™.

3. Results and discussion

3.1. Reference samples

3.1.1. Colorimetric measurements

The colour parameters of the reference samples projected on the a*b* plane of the CIE L*a*b* colour space are shown in Fig. 2.

The red, orange and pink samples clustered at relatively high values

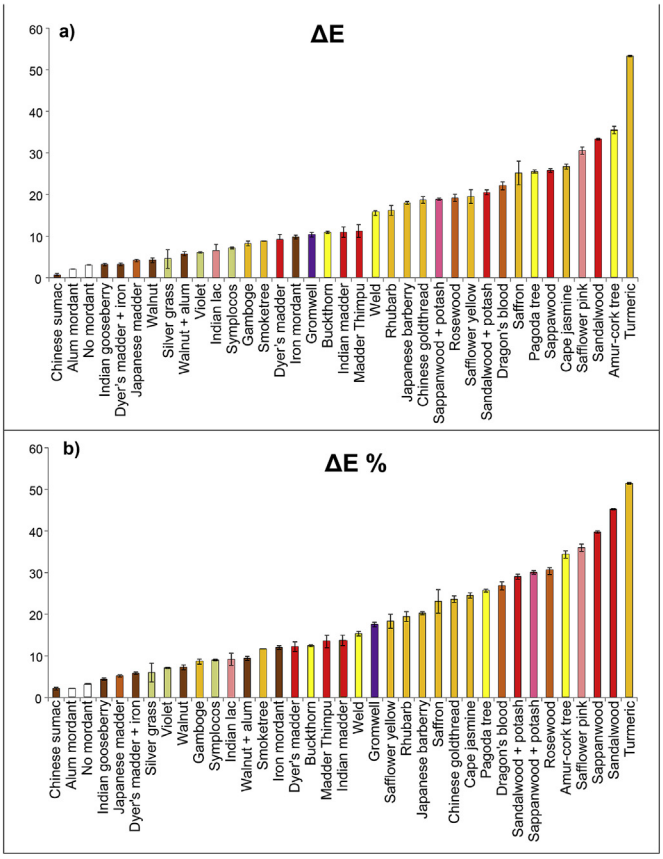

Fig. 3. a) ΔE and **b)** ΔE % values obtained after ageing of the reference samples as a histogram, showing the increasingly light-sensitive nature of the dyes investigated.

of a* and the samples with intense yellow colours clustered at high values of b*. Buckthorn, weld, pagoda tree and amur-cork tree showed negative values of a*, indicative of a slight green hue in these samples. Symplocos, silver grass and violet were lightly coloured and with a slight brown hue, which contributed to their grouping with the other brown samples. Four pairs of samples were created to evaluate the colour difference induced by changing some parameters in the dyeing procedure. Walnut husks extracts were used to dye both non-mordanted and alum-mordanted silk. The colour obtained was very similar, indicating that the mordanting is not necessary for this dye and does not play an important role in the final hue. Dyer's madder extracts were used to dye both alum-mordanted and iron-mordanted silk. In this case the colour difference was significant: an expected red/orange colour was obtained with the alum mordant and a brownish red was obtained with iron. Sappanwood and sandalwood extracts were used to dye at neutral and alkaline pH, as the final hue is reported to be pH-dependent [59]. For sappanwood a remarkable difference was observed: a bright red colour was obtained at neutral pH and a bright fuchsia at alkaline pH. For sandalwood the red colour obtained at alkaline pH was more brownish than the one obtained at neutral pH.

In addition to describing the colours obtained, colorimetric measurements were used to evaluate the extent of fading and/or the colour changes induced by artificial ageing (light exposure). Table S3 (Supplementary Information) reports the colorimetric parameters (L*, a* and b*) measured before and after ageing, together with the corresponding ΔL*, Δa* and Δb*, and the calculated ΔE. The colour parameters of the aged reference samples projected on the a*b* plane of the CIE L*a*b* colour space are also shown in Fig. 2. Generally, a decrease in the a* values and a decrease in the b* values were observed for most red and yellow dyes, respectively, in agreement with a loss of the red and yellow components of the colour, respectively.

In order to also consider the variations in the L* component, ΔE values were evaluated. Fig. 3a shows the ΔE values as a histogram. Three reference samples of non-mordanted, alum-mordanted and iron-mordanted silk were included in order to gauge the effects of ageing of the fabric itself. Slight colour changes were detected for the non-mordanted and alum-mordanted samples, mainly related to a decrease in the b* component (yellowing), resulting in ΔE values $\leq$ 5. For the iron-mordanted fabrics, which showed a significant brown colouration, more relevant changes were observed, involving a decrease in the L* and b* components, thus indicating a darkening and yellowing of the fabric, which resulted in a ΔE value around 10.

In terms of dyed textiles, the brown samples (Indian gooseberry, walnut and Chinese sumac) and the madder samples showed low ΔE values, indicating good lightfastness of these dyes, in agreement with previous studies [29]. Good lightfastness was also shown by Indian lac. All the other red/orange/pink dyes from rosewood, dragon's blood, sandalwood, sappanwood and safflower pink showed high values of ΔE (*ca.* 20–30) [33,34]. A high contribution was generally given by a positive ΔL*, indicative of a general loss of colour and a negative Δa*, indicative of a predominant loss of the red component. For dragon's blood and safflower pink a significant negative Δb* (due to a loss of yellow components) was also observed. Notably, although the ΔE for gromwell was not very high (*ca.* 10), the colour underwent quite a drastic change, turning from purple to a brownish purple, mainly due to a positive Δb* (yellowing). Among the yellow dyes, symplocos, violet and silver grass showed the lowest ΔE, but this result is probably related to the fact that the colouration of the fabric was quite weak before ageing. On the other hand, buckthorn, weld, smoketree and gamboge, which produced bright colourations, showed ΔE $\leq$ 15, mainly due to a negative Δb* (loss of yellow components), and can therefore be considered of relatively good lightfastness. All the other yellow dyes showed ΔE $\geq$ 20, with turmeric showing an almost complete loss of colour (ΔE $>$ 50), in agreement with other studies [33].

On a general note, it appeared that in most cases the samples with higher a* and b* values lost or changed colour to a higher extent, resulting in a higher ΔE. Considering the different starting point in terms of colour components of these samples, there is a risk that the ΔE value would not be completely representative of the actual light-sensitivity of these dyes. In fact, although useful to compare the initial and final colour of a sample, ΔE is probably not the best parameter to compare among very different samples. We therefore decided to normalise ΔE for the initial colour values and we calculated ΔE %, by dividing the ΔE by the square root of $(L^*)^2 + (a^*)^2 + (b^*)^2$ before ageing. The values obtained are presented as a histogram in Fig. 3b and are reported in Table S3 (Supplementary Information). It emerged that the order of light-sensitivity of these dyes was slightly different. The brown dyes, Indian lac, madder dyes, silver grass, symplocos, violet, gamboge, smoketree, buckthorn and weld confirmed their relatively good lightfastness. Gromwell showed a ΔE % of *ca.* 20%, which was more in agreement with the colour change observed. Rosewood and dragon's blood also appeared more light-sensitive than what observed without normalisation. For the other dyes, apart from some minor differences, the extent of colour change was confirmed. Turmeric, sappanwood, sandalwood and safflower pink were the most light-sensitive dyes, and the results were mostly in agreement with other previous studies [29,33,34].

3.1.2. Multispectral imaging

Figs. 4 and 5 report the visible-reflected (VIS), ultraviolet-luminescence (UVL), infrared-reflected false colour (IRRFC) and ultraviolet-reflected false colour (UVRFC) images obtained for the reference samples before and after ageing.

The VIS images are a visual summary of what was described in the previous section, as they clearly show the significant fading of certain dyes, in particular rosewood, dragon's blood, sandalwood, sappanwood,

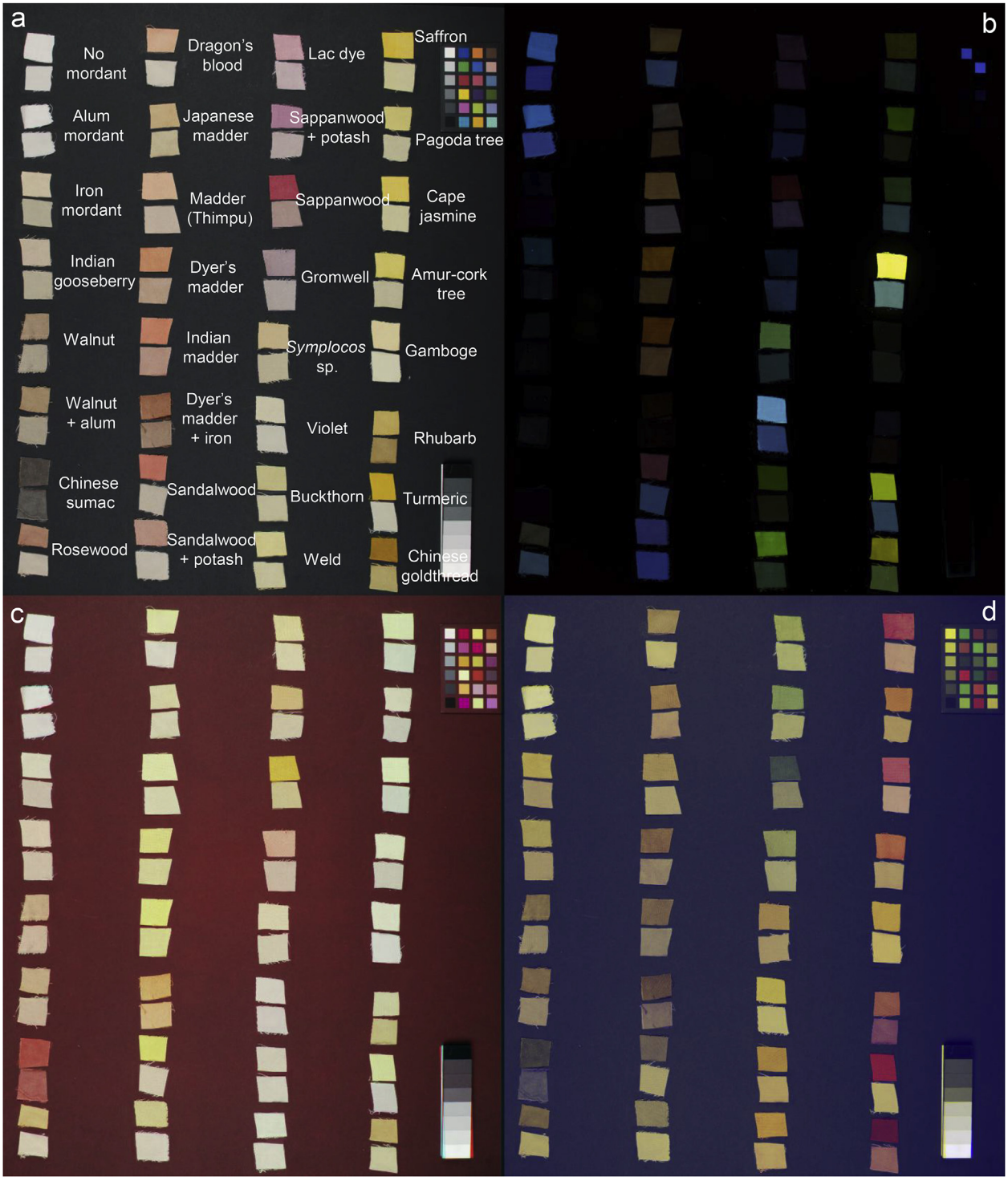

Fig. 4. a) Visible-reflected (VIS), b) ultraviolet-luminescence (UVL), c) infrared-reflected false colour (IRRFC) and d) ultraviolet-reflected false colour (UVRFC) images obtained for the reference samples. The samples are shown as pairs: for each pair the upper samples are non-aged and the lower samples are aged. (For interpretation of the references to colour in this figure legend, the reader is referred to the Web version of this article.)

safflower, as well as most of the yellow dyes, especially turmeric.

The UVL images of the samples before ageing were extremely valuable in highlighting characteristic emission or absorption properties of some of the dyes investigated. The non-mordanted and alum-mordanted silk exhibited blue luminescence, which is common for proteinaceous materials [60]. All the brown dyes absorbed the UV radiation, appearing dark in the images. All the madder samples, except for the iron-mordanted one, showed a characteristic pink/orange luminescence (relatively low), which is known to be typical of this group of dyes [61]. Pink safflower also showed a relatively intense orange luminescence [62]. Sandalwood and sappanwood produced a weak red luminescence. Among the yellows, the protoberberine-based dyes, such as amur-cork tree, Chinese goldthread and Japanese barberry, exhibited an intense yellow luminescence, with the amur-cork tree appearing most intense [63]. Turmeric emitted in the yellow-green part of the spectrum [64]. Pagoda tree, smoketree and yellow safflower also produced a weak

Fig. 5. a) Visible-reflected (VIS), b) ultraviolet-luminescence (UVL), c) infrared-reflected false colour (IRRFC) and d) ultraviolet-reflected false colour (UVRFC) images obtained for the reference samples. The samples on the left are non-aged and the samples on the right are aged. (For interpretation of the references to colour in this figure legend, the reader is referred to the Web version of this article.)

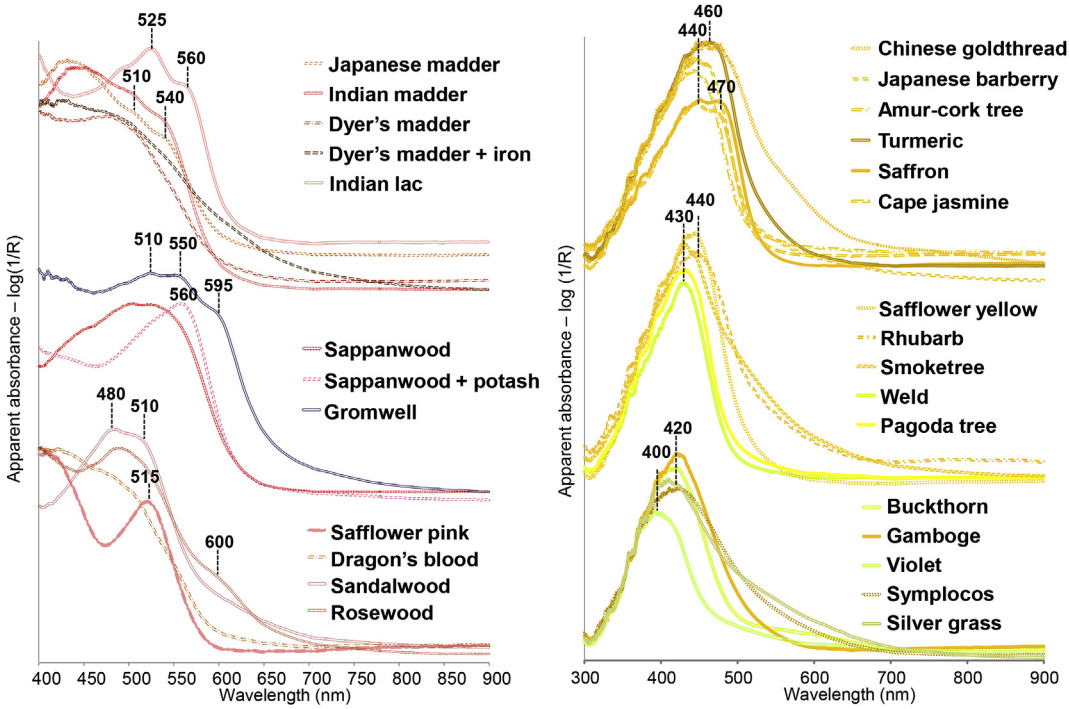

Fig. 6. FORS spectra (apparent absorption) of the reference dye samples.

yellow-green luminescence. Some green hues were additionally obtained for symplocos, weld and buckthorn. A blue contribution from the silk to these green emissions is probably significant. Visible-induced visible luminescence (VIVL) images were very useful in this regard. These images are recorded by illuminating the sample using blue light and collecting the luminescence emitted in the yellow-red region of the visible spectrum. The longer excitation wavelength compared to UV avoids the absorption maximum of most fibres [60], suppressing the background luminescence and minimising the colour-modifying effects [57]. Thus, in the VIVL images (Figure S1, Supplementary Information) the reference samples appear dark, as well as the non-emitting samples, such as all the browns, saffron and cape jasmine. All the other samples show some luminescence, in agreement with what observed in the UVL images, but distinguishing between the hues was not straightforward. The method is therefore useful in highlighting luminescing materials with no interference from the background, but for the dyes investigated appears less informative than UVL for diagnostic purposes.

Generally, fading after artificial ageing resulted in a weakening of the luminescence observed from the dyes, leading to an increased blue contribution from the silk in UVL images and weaker emissions in VIVL images.

IRR images (not shown) showed that all the samples were mainly

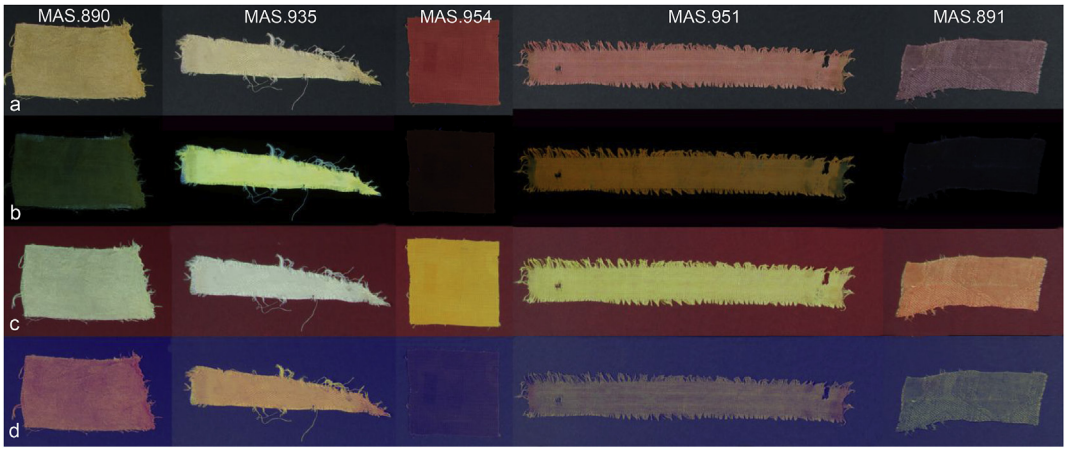

Fig. 7. a) Visible-reflected (VIS), b) ultraviolet-luminescence (UVL), c) infrared-reflected false colour (IRRFC) and d) ultraviolet-reflected false colour (UVRFC) images obtained for the monochrome textiles MAS.890, MAS.935, MAS.954, MAS.951 and MAS.891. (For interpretation of the references to colour in this figure legend, the reader is referred to the Web version of this article.)

transparent to this component of the radiation. These data were used to create false colour images (IRRFC), where the actual differences in transparency can be better appreciated, as they contribute to create different colours. In fact, most of the samples appeared a yellow hue, indicating a weak absorption of the IR radiation, whereas Chinese sumac appeared red, indicating a total transparency. Gromwell appeared orange, and was thus distinctively different from all the other samples.

UVR images (not shown) highlighted some interesting absorption properties in this part of the spectrum. In particular, Chinese sumac, iron-mordanted madder, buckthorn, weld, pagoda tree, gamboge, turmeric and Chinese goldthread appeared very dark in these images. When false-colour images were created, Chinese sumac appeared brown and the madder samples also showed a brownish hue. Green was observed for lac, sappanwood and gromwell and red hues for saffron, cape jasmine, turmeric and Chinese goldthread. The other yellow samples showed a yellow hue.

A summary of the response exhibited by each reference sample in the various multispectral images is reported in Table 2.

3.1.3. FORS

As described in Aceto et al. [49], apparent absorption spectra (Kubelka–Munk or log(1/R) conversion of reflectance data) are more relevant than reflectance spectra to the identification of organic colourants, as the positions of the absorption features are generally more constant and maxima are more informative than reflectance features.

Fig. 6 shows the apparent absorption spectra (log(1/R) of reflectance data) obtained from FORS analysis of the reference samples. The brown samples (Indian gooseberry, walnut and Chinese sumac; not shown) produced broad absorption bands with no characteristic features. Among the madder samples, Japanese madder and Indian madder showed the characteristic absorption maxima at around 510 and 540 nm [49–52]. However, the spectra obtained for the samples of dyer's madder, both alum- and iron-mordanted, did not show a clear structure. Examples of this related to dyeing procedure, origin of raw materials or dye concentration effects have been noted in the literature [50,52,57]. The iron-mordanted sample showed a broader absorption feature, particularly in the red region of the spectrum, in agreement with a change in the position of the inflection point associated with the steep increase in reflectance in the red portion of the visible spectrum, and the corresponding colour change [50]. The Indian lac sample produced a characteristic spectrum generally obtained for insect-based red dyes (kermes, cochineal and lac) with two absorption maxima at *ca.* 525 and 560 nm [49]. The spectrum obtained for the sappanwood sample extracted at neutral pH produced a relatively broad absorption with a maximum at *ca.* 530–540 nm, in agreement with the results present in Ref. [52]. For the sappanwood sample extracted at alkaline pH, the absorption maximum was shifted to *ca.* 560 nm and showed a narrow absorption profile, more in agreement with previously published data [49]. A very defined and characteristic FORS spectrum was also obtained for safflower pink, whose sharp absorption maximum was at *ca.* 520 nm, in agreement with previous findings [52,62]. On the contrary, dragon's blood did not produce a structured spectrum [49], with absorption features mainly concentrated below 500 nm. For the other red samples (rosewood and sandalwood) no literature data were available at the time of publication. The spectrum for the rosewood showed two absorption features: a main one with a maximum at *ca.* 490 nm and a second one at *ca.* 600 nm. The spectra obtained from the sandalwood samples extracted at neutral and alkaline pH were very similar, showing an absorption band with two poorly resolved maxima at *ca.* 480 and 510 nm. Gromwell produced a very distinctively structured spectrum with three maxima at *ca.* 510, 550, 595 nm.

As regards the yellow dyes, it is reported that their identification using FORS is difficult [49], as their main absorption feature is a band at *ca.* 400–450 nm, whose position does not change significantly among these dyes. However, some differences were observed in the data obtained from the yellow reference samples. The results for the three protoberberine-based dyes (amur-cork tree, Japanese barberry and Chinese goldthread) and turmeric showed a maximum at higher wavelength compared to the other samples (*ca.* 445–460 nm). The absorption maximum for saffron and cape jasmine showed some structure, resulting in two poorly resolved maxima at *ca.* 445 and 470 nm, in agreement with the behaviour of carotenoids [45,50]. Safflower yellow, rhubarb, smoketree, pagoda tree and weld produced a maximum between 420 and 440 nm. Buckthorn, gamboge, violet, symplocos and silver grass produced a maximum between 400 and 420 nm. It is difficult to ascertain how significant these differences are, as slightly different values are found in the literature and absorption features are reported to vary depending on the dye preparation methods [49,50].

The main absorption features observed for the dyes under investigation are summarised in Table 2 together with the colour combinations shown in the multispectral images.

3.2. Archaeological textiles

By comparing the results and observations obtained on the archaeological textiles with the database created using the reference samples (Table 2), a preliminary identification of some of the dyes was possible. These results are summarised in Table 3 and discussed in the following sections.

Table 3
Summary of the results obtained by FORS and multispectral imaging for the textiles investigated. Question marks (?) indicate uncertainty in the identification.

Object	Colour	FORS (nm)	UVL	IRRFC	UVRFC	Results
Monochrome woven silk textiles						
MAS.890	yellow	430	olive	white	orange	unidentified
MAS.935	yellow	440	bright yellow	white	orange	protoberberine-based
MAS.936	yellow	415	yellow	white	orange	protoberberine-based (probably low concentration)
MAS.938	yellow	415, 525	dark yellow	white	orange	faded safflower and unidentified yellow
MAS.942	yellow	410	light yellow	white	orange	unidentified
MAS.904	orange	515	orange	yellow	brown	safflower
MAS.951	orange	515	bright orange	yellow	brown	safflower
MAS.939	red	not structured	dark	yellow	dark	unidentified
MAS.954	red	510, 540	dark	yellow	brown	plat-based red, probably madder
MAS.896	brown	510, 555, 595	dark	red	green	gromwell
MAS.949	brown	510, 550, 595	dark	orange	green	gromwell
MAS.891	purple	510, 550, 595	dark	orange	green	gromwell
MAS.900	purple	510, 550, 595	dark	orange	green	gromwell
MAS.901	purple	510, 550, 595	dark	orange	green	gromwell
MAS.902	purple	510, 550, 595	dark	orange	green	gromwell
MAS.903	purple	510, 550, 595	dark	orange	green	gromwell
MAS.937	purple	510, 550, 595	dark	orange	green	gromwell
Polychrome woven silk textiles						
MAS.865	orange	515	orange	yellow	brown	safflower
	yellow	420	olive	white	red	unidentified (carotenoid?)
	blue	660	blue	red	green	indigo
	light blue	660	light blue	pink	aqua	indigo
MAS.869	orange	515	orange	yellow	brown	safflower
	yellow	420	olive	white	orange	unidentified
	green	420, 660	dark green	pink	brown	unidentified yellow and indigo
	purple	510, 550, 595	dark	orange	green	gromwell
MAS.871	red	515	orange	yellow	brown	safflower
	purple	510, 550, 595	dark	orange	green	gromwell
	yellow	415	olive	white	orange	unidentified
	green	420, 660	blue	pink	green	unidentified yellow and indigo
	pink	515	orange	white	green	safflower
MAS.872	yellow	430	yellow	lemon yellow	red	unidentified (carotenoid?)
	green	420, 660	green	pink	brown	unidentified yellow and indigo
	red	540 (not structured)	red	yellow	brown	sappanwood ?
	red back	540 (not structured)	orange	yellow	brown	sappanwood ?
	blue	660	blue	pink	green	indigo
MAS.873	yellow	425	olive	lemon	red	unidentified
	green	420, 660	dark	red	brown	unidentified yellow and indigo
	orange	515	orange	yellow	brown	safflower
	red back	515	orange	yellow	brown	safflower
	blue	660	blue	pink/red	green	indigo
MAS.906.a-b	yellow 1	430	olive	yellow	brick red	unidentified
	yellow 2	435	yellow	orange	brown	protoberberine-based
	green	430, 660	olive	pink	brown	unidentified yellow and indigo
	orange	420, 515	orange	yellow	brown	unidentified yellow and safflower
	blue	660	blue	pink/red	green	indigo
	pink	420, 515	yellow	pale yellow	brown	unidentified yellow and safflower
	brown	broad absorption	dark	brown	brown	tannins
	purple	510, 550, 595	dark	orange	green	gromwell
MAS.908.a-b	pink	not structured	pink	pale yellow	brown	unidentified
	yellow	440	yellow	orange	red	protoberberine-based
	green	440, 660	olive	pink	brown	unidentified yellow and indigo
	brown	broad absorption	dark	brown	brown	tannins
	blue	660	blue	pink/red	green	indigo
	light blue	660	light blue	pink	yellow	indigo
MAS.920	yellow	425	olive	white	orange	unidentified
	pink	515	orange	yellow	brown	safflower
	blue	660	blue	pink/red	green	indigo
MAS.922	red	540 (not structured)	dark	orange	purple	sappanwood ?
	yellow	420	pale yellow	white	orange	unidentified
	pink	51	orange	yellow	light purple	safflower
	blue	660	blue	pink/red	green	indigo
MAS.924	yellow	420	olive	pale yellow	orange	unidentified
	green	420, 660	green	pink	brown	unidentified yellow and indigo
	beige	featureless	grey	yellow	brown	unidentified
	blue	660	blue	pink/red	green	indigo
MAS.929	yellow	420	pale yellow	white	orange	unidentified
	black	broad absorption	dark	red	brown	tannins
Embroidered silk textiles						

(*continued on next page*)

Table 3 (*continued*)

Object	Colour	FORS (nm)	UVL	IRRFC	UVRFC	Results
MAS.911	brown (ground)	510, 540	dark	orange	brown	plat-based red (madder) and tannins ?
	brown (embroidery)	510, 540	dark	orange	brown	plat-based red (madder) and tannins ?
	blue	660	blue	pink/red	green	indigo
	green	420, 660	lemon yellow	pink	brown	protoberberine-based yellow and indigo
	pink	featureless	pale orange	yellow	beige	safflower ?
	orange (back)	520	orange	yellow	brown	safflower
MAS.915	red	poorly structured	dark	orange	purple	plat-based red, probably madder ?
	pink	515	orange	yellow	brown	safflower
	light green	440, 660	green	pink	brown	protoberberine-based yellow and indigo
	dark green	440, 660	dark green	red	dark	protoberberine-based yellow and indigo
	blue	660	blue	pink/red	green	indigo
	light blue	660	light blue	pink	light green	indigo
MAS.1130	yellow1	420	lemon yellow	white	orange	protoberberine-based yellow
	yellow2	420	yellow	white	orange	protoberberine-based yellow
	light yellow	featureless	beige	pale yellow	brown	unidentified
	dark green	420, 660	green	pink	brown	unidentified yellow and indigo
	green	420, 660	light green	pink	brown	unidentified yellow and indigo
	brown/red	510, 540	dark	orange	brown	plat-based red (probably madder) and tannins
	red	510, 540	dark	orange	purple	plat-based red, probably madder
	pink	525, 565	dark	yellow	green	insect-based red
	purple	510, 540, 660	dark	orange	purple	plat-based red (probably madder) and indigo
	blue	660	blue	pink/red	green	indigo
	light blue	660	light blue	pink	light green	indigo

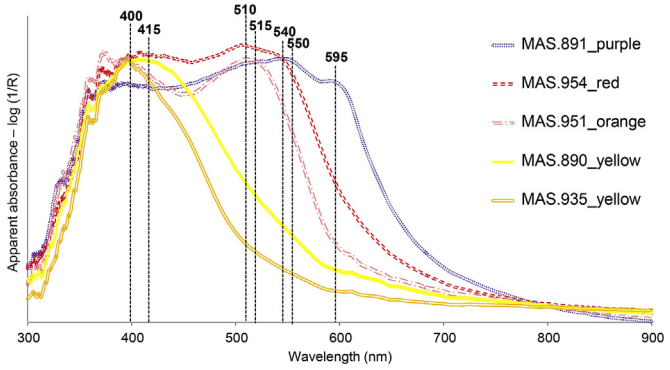

Fig. 8. FORS spectra (apparent absorbance) of monochrome textiles MAS.891 (gromwell), MAS.954 (plant-based red, probably madder), MAS.951 (safflower), MAS.890 (unidentified yellow) and MAS.935 (protoberberine-based yellow). The corresponding textiles are shown in Fig. 7. (For interpretation of the references to colour in this figure legend, the reader is referred to the Web version of this article.)

3.2.1. Monochrome textiles

Out of the seventeen monochrome textiles investigated, five representative groups emerged from the multispectral imaging sets acquired and these are shown in Fig. 7.

One of the yellow textiles (MAS.935) exhibited a bright yellow luminescence in the UVL image. All the other yellow textiles showed a much weaker yellow-green luminescence, as for MAS.890. Very pale yellow colours were observed in the IRRFC images and slightly different nuances of orange in the UVRFC images of all the yellow textiles. FORS spectra also produced two main results: an absorption maximum at *ca.* 400 nm for MAS.935 and absorption maxima at *ca.* 410–420 nm for all the other yellow textiles, as shown in Fig. 8. The bright luminescence of MAS.935 pointed towards a protoberberine-based dye. The colour appeared to be more in agreement with the amur-cork tree dye rather than the Japanese barberry or the Chinese goldthread. However, the absorption feature obtained by FORS did not match any of the results obtained for these species. As previously mentioned, the exact position of the absorption maximum for yellow dyes is not very reliable and degraded fibres themselves can contribute to the yellow colour. As regards the other yellow textiles, the results were not conclusive. A weak yellow-green luminescence is common to many sources of dyes, as well as an absorption maximum at 410–420 nm in the FORS spectra.

MSI of the red-orange textiles also produced two main categories of results. On one hand, MAS.951 (Fig. 7) and MAS.904 exhibited a bright orange luminescence in UVL images, light yellow colouration in IRRFC images and a brownish hue in UVRFC images, whereas MAS.954 (Fig. 7) and MAS.939 appeared a weak red-orange in UVL images, deep yellow in IRRFC and dark brown in UVRFC. FORS spectra of MAS.951 and MAS.904 showed a sharp absorption maximum at *ca.* 515 nm (Fig. 8), which, in combination with the MSI observations, enabled the clear identification of red safflower in these textiles. The FORS spectrum of MAS.954 showed two absorption maxima at *ca.* 510 and 540 nm, which are consistent with the presence of a plant-based red, probably madder (*Rubia* spp) considering the geographical provenance. Moreover, a slightly brighter luminescence was obtained for the reference madder samples with comparison to this textile, but it has been already proposed that high concentrations of madder dye can result in the attenuation of the luminescence intensity observed [57]. The FORS spectrum of MAS.939 (not shown) showed a less clear structure, although two weak absorption maxima could be observed at *ca.* 510 and 540 nm, therefore also suggesting a plant-based red, probably madder.

All the purple textiles (MAS.891, MAS.900, 901, 902, 903, 937) and the more brown-coloured ones (MAS.896 and MAS.949) showed similar results. They mainly absorbed UV radiation and therefore appeared dark in UVL images, whereas deep orange and green colours were observed in the IRRFC and UVRFC images, respectively (Fig. 7). All of them also produced FORS spectra with three absorption maxima at *ca.* 510, 550 and 595 nm (Fig. 8), which enabled gromwell to be confirmed as the source of purple colour. The fading of gromwell to a brownish hue was also in agreement with our ageing experiments.

3.2.2. Polychrome textiles

An additional level of complexity was added to the interpretation of the MSI images of the polychrome textiles, each containing many combinations of colours. The acquisition and interpretation of the FORS spectra were also more difficult, due to the weave of some textiles and the thinness of some coloured areas. Most textiles showed different motifs and colours on the front and back, which resulted in contributions from the colours on the back to the FORS spectra of the colours on the front and vice versa (Figure S2a-b, Supplementary Information).

MAS.869 and MAS.922 are two examples of the importance of investigating both the back and the front of these textiles. In addition to the different designs and colours present, the effects of fading of these

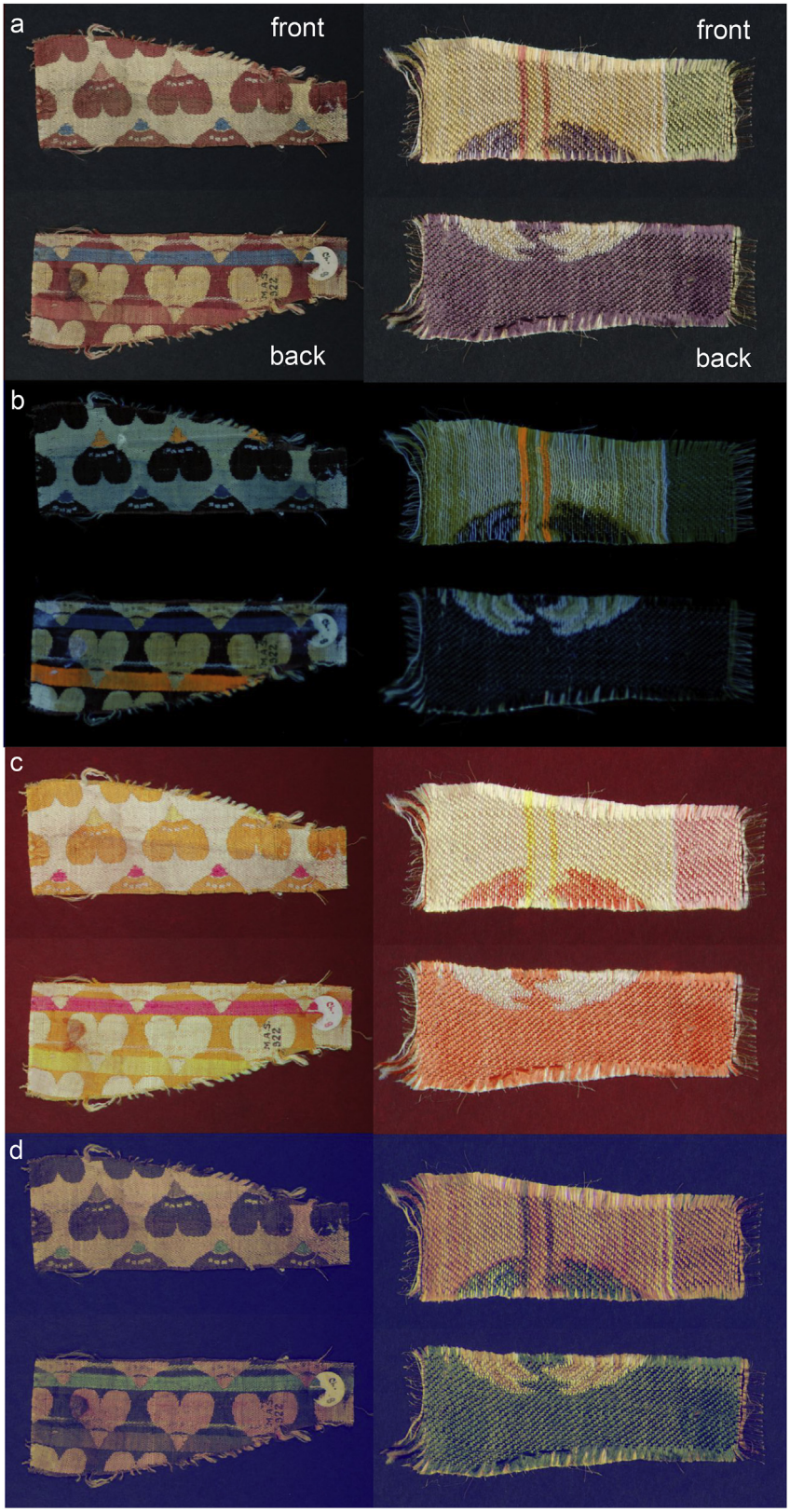

Fig. 9. a) Visible-reflected (VIS), b) ultraviolet-luminescence (UVL), c) infrared-reflected false colour (IRRFC) and d) ultraviolet-reflected false colour (UVRFC) images obtained for MAS.922 (left) and MAS.869 (right). The front (top) and back (bottom) of the textiles are present in each image. MBR and VIVL images are shown in Figure S3 (Supplementary Information). (For interpretation of the references to colour in this figure legend, the reader is referred to the Web version of this article.)

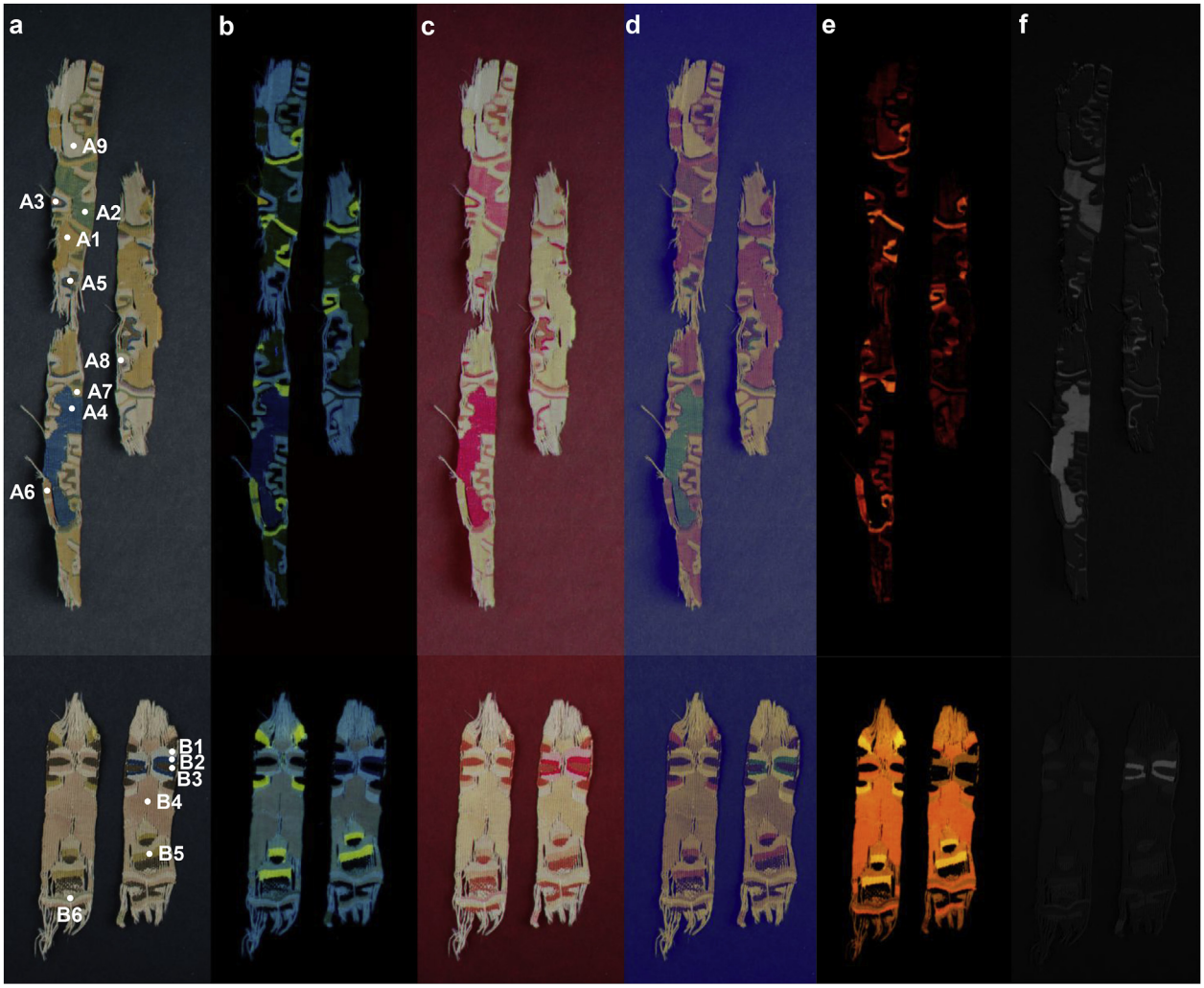

Fig. 10. a) Visible-reflected (VIS), b) ultraviolet-luminescence (UVL), c) infrared-reflected false colour (IRRFC), d) ultraviolet-reflected false colour (UVRFC), e) visible-induced visible luminescence and f) multi-band reflected images obtained for MAS.906-ab (top) and MAS.908-ab (bottom). The areas where FORS measurements were taken are indicated. (For interpretation of the references to colour in this figure legend, the reader is referred to the Web version of this article.)

colours must also be considered. The VIS images of MAS.922 (Fig. 9) clearly show how the pink and yellow are more intense on the back than on the front (details in Figure S2d-e, Supplementary Information). In the UVL images the bright orange luminescence, corresponding to the pink areas of MAS.922 and the red stripes of MAS.869, revealed the presence of safflower, confirmed by its distinctive sharp absorption maximum at *ca.* 515 nm in the FORS spectra. The red colour of the petals in MAS.922 appeared to mostly absorb the UV radiation and produced an unstructured FORS spectrum with an absorption feature at relatively long wavelengths (*ca.* 545 nm), which could point towards the presence of sappanwood (Fig. 12). The distribution of the yellow colour in the front of MAS.869 (as white and yellow threads alternating in this area of the textile, Figure S2c, Supplementary Information) appeared clearer in the UV image. The yellow colour exhibited a weak olive emission in the UVL image, which, when compared with the reference samples, could point towards cape jasmine, saffron or pagoda tree as possible sources. The lack of features in the corresponding FORS spectrum suggested the pagoda tree as most probable option, as cape jasmine would have shown two maxima (445 and 470 nm) according to the results obtained on the reference samples (Table 2). However, this is very hypothetical based only on these results.

IRRFC images showed a bright yellow colour in correspondence with the safflower areas and a deep red-orange for the purple areas in MAS.869, indicative of the presence of gromwell, as confirmed by its three distinctive absorption maxima at *ca.* 510, 550 and 595 nm in the FORS spectra. IRRFC images were also useful to map the presence of indigo, both alone and in mixtures with other dyes. The blue areas of MAS.922, in fact, appeared a bright fuchsia colour in the IRRFC images, which is typical of indigo [57]. Lighter shades of pink were obtained when indigo is mixed with yellow to obtain green colours, as for MAS.869. In the UVRFC images both purple and blue areas appeared green, which made the distinction between gromwell and indigo difficult from this image alone. Another useful way of mapping the distribution of indigo is multiband-reflected (MBR) imaging [57]. Indigo-containing areas appear white in MBR images. Generally, this is also true for indigo mixed with other dyes. Therefore, information about mixtures is lost if compared with IRRFC, but a mixture of a plant-based red (probably madder) and indigo can be potentially distinguished from gromwell, as the latter appears a dull grey in MBR images. Nevertheless, attention must be paid, as the concentration of the dyes can influence the final white/grey shade observed in the processed image. MBR images of MAS.869 and MAS.922 are shown in Figure S3 (Supplementary Information), and some examples of other textiles are reported in Figs. 10 and 11. The presence of indigo in the blue and green areas was finally confirmed by the characteristic absorption at *ca.* 660 nm in the FORS spectra.

MAS.906a-b and MAS.908a-b were more complex textiles. Woven with a different technique, known as *kesi*, the designs present very

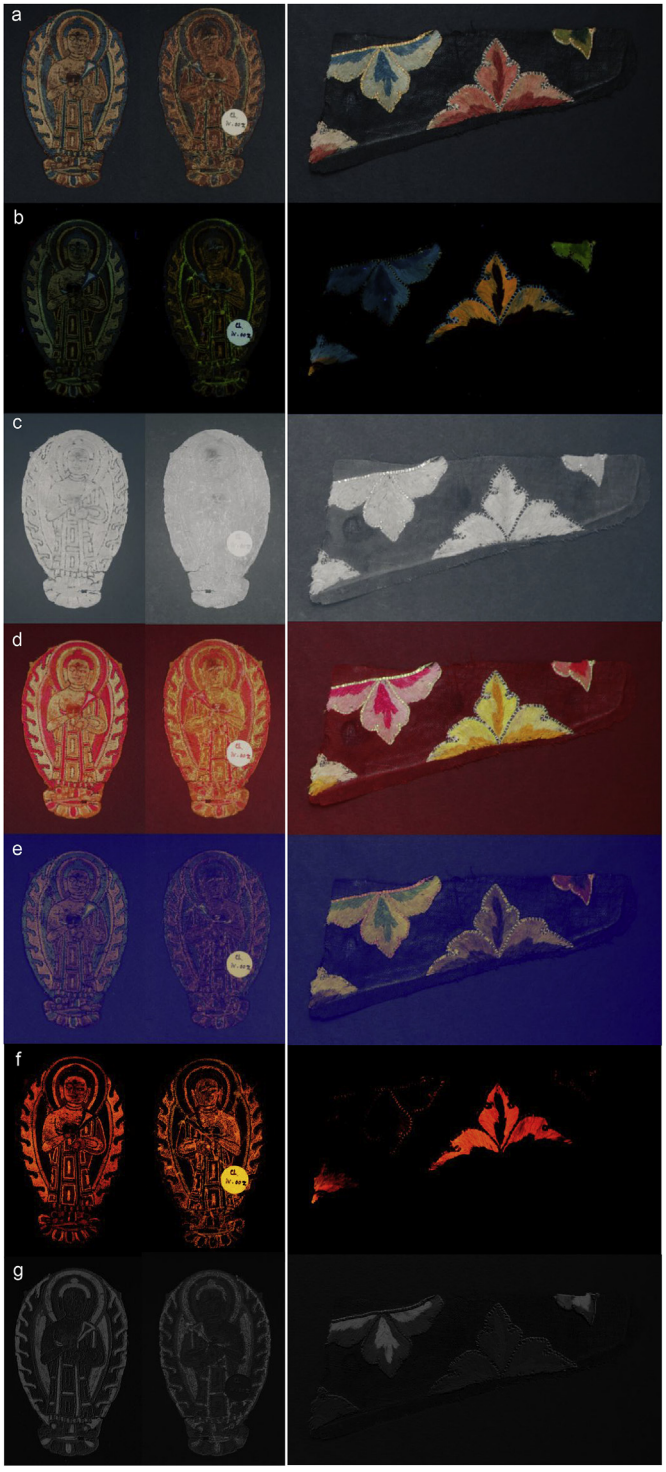

Fig. 11. a) Visible-reflected (VIS), b) ultraviolet-luminescence (UVL),c) infrared-reflected (IRR) d) infrared-reflected false colour (IRRFC) and e) ultraviolet-reflected false colour (UVRFC) images obtained for the front and back of MAS.911 (left) and MAS.915 (right). (For interpretation of the references to colour in this figure legend, the reader is referred to the Web version of this article.)

narrow stripes composed of different colours, as observed by digital microscopy (Figure S4, Supplementary Information). The very thin (200–300 μm) nature of some of these stripes meant that the FORS measurements unavoidably contained contributions from neighbouring areas, as the FORS probe has a diameter of *ca.* 1 mm. The areas where FORS measurements were taken are shown in Fig. 10.

Also in this case, UVL images were extremely informative. Two different sources of yellow, which were not distinguishable in VIS images, were evident in MAS.906a-b. Yellow1 (A1, Fig. 10) appeared an olive colour in the UVL image and showed an absorption maximum at *ca.* 430 nm, possibly in agreement with the pagoda tree dye. Yellow2 (A7, Fig. 10) exhibited yellow luminescence and an absorption maximum at *ca.* 430 nm, typical of the amur-cork tree dye. Similar observations as those made for yellow2 were noted for the yellow colour in MAS908-ab.

A bright orange area (A3, Fig. 10) and a pinker one (A6, Fig. 10) were also present in MAS.906a. Both these areas showed an intense yellow-orange luminescence in the UVL images, which may possibly be produced from a mixture of a protoberberine-based yellow and safflower. This hypothesis was confirmed by FORS, as the spectra obtained revealed the presence of safflower mixed with a yellow dye (absorption maxima at *ca.* 440 and 515 nm, Fig. 12). On the other hand, the pink colour of MAS.908-ab (B4, Fig. 10) did not show the bright luminescence typical of safflower and the FORS spectrum appeared unstructured, making faded sappanwood a possible hypothesis for the dye used in these areas. The VIVL images showed the luminescing dyes in these textiles even more clearly than the UVL images, especially regarding the contrast between the two different yellows in MAS.906a-b. The pink colour of MAS.908-ab actually appeared quite luminescent in the VIVL images, and the hue was consistent with faded sappanwood (Figure S1, Supplementary Information).

Gromwell was again identified as the source of the purple stripes in MAS.906b from the typical orange and green colours observed in IRRFC and UVRFC images, respectively, as well as the FORS spectrum showing the three absorption maxima at *ca.* 510, 550 and 595 nm. Indigo was mapped in the IRRFC in both blue and green areas appearing different shades of pink and its presence was confirmed by the typical absorption at *ca.* 660 nm in FORS spectra. These textiles also represented a nice example of the potential of multiband-reflected (MBR) images in mapping the distribution of indigo.

Finally, brown areas and stripes were present on these textiles. The dye used to obtain the colour exhibited absorption in both the UV and IR ranges, which made these areas appear dark in the corresponding UVL, UVR and IRR images (IRR image not shown). As a consequence a dull orange-brown was obtained in IRRFC images and dark brown in UVRFC images. This, together with quite a featureless FORS spectrum, was indicative of the presence of tannins used to obtain these brown colours [57].

3.2.3. Embroideries

Embroidered textiles can be even more complex in terms of non-invasive investigations, as stitches are applied on a textile ground. Thus, separating the information coming from the two layers can be challenging. In our cases, mainly brown and black grounds were used, which made interferences less significant.

The multispectral images obtained for MAS.911 and MAS.915 are shown in Fig. 11. MAS.911 was another interesting example of the effects of fading on the appearance of a textile. The figure of the Buddha appeared very lightly coloured on the front, whereas a much brighter pink/orange hue was evident on the back (details in Figure S5, Supplementary Information). UVL images revealed the presence of safflower, confirmed by FORS, but only as a result of the access to the back of the object, where this was less faded. Similarly, the presence of safflower was evident in the pink areas of the red flowers of MAS.915. The aqua colour in MAS.911 also appears greener on the back than on the front. A mixture of indigo and yellow was identified by FORS, and the yellow component exhibited a bright yellow luminescence in the UVL images, enabling it to be identified as a protoberberine-based dye. Similar results were obtained for the green flower in MAS.915. Both the light and dark areas were luminescent, showing a green hue. The observed colour was influenced by the luminescence of silk, as visible from the VIVL images, and the presence of indigo can also partially

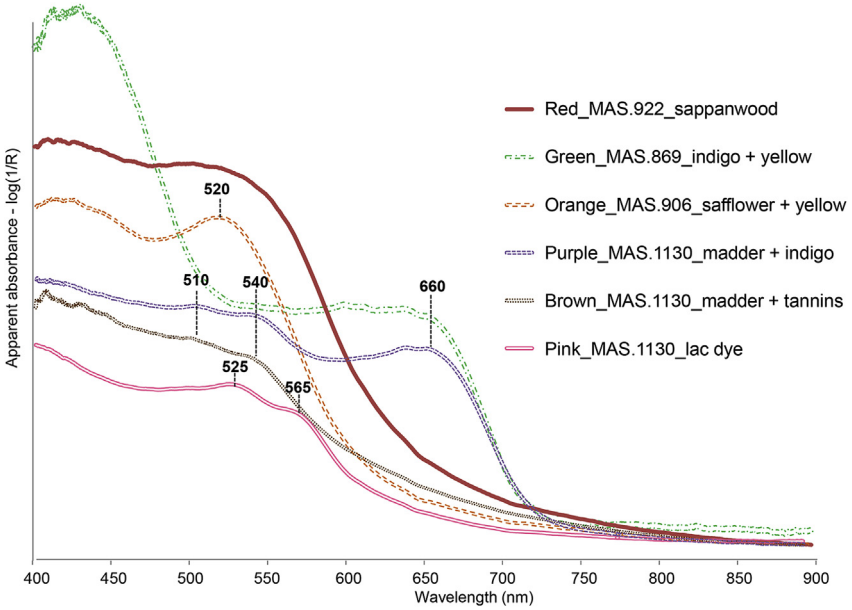

Fig. 12. FORS spectra (apparent absorbance) of some particular coloured areas in textiles MAS.869, MAS.906, MAS.922 and MAS.1130.

contribute to the green hue. It is therefore difficult to hypothesise which kind of protoberberine-based dye is more likely to be present, although Japanese barberry shows the greenest luminescence. The brown background in MAS.911 was likely obtained with a tannin-based dye, as suggested by the high absorption of the UV radiation. However, the FORS spectrum suggested the presence of a plant-based red (probably madder), possibly in a mixture with the tannins, as two weak absorption maxima at *ca.* 510 and 540 nm were present.

The IRR images of MAS.911 and MAS.915 also showed an interesting result, as dark outlines were visible on both textiles, suggesting the presence of an IR-absorbing material. Digital microscopy (Figure S5, Supplementary Information) helped to reveal the gilding of these areas. However, rather than the use of gold threads, the gilding appeared to have been applied as a leaf on the top of silk threads using a black material, which was visible where the gilding was missing. This was the IR-absorbing, likely carbon-based, material and further investigations will be performed to identify it and better understand this decorative technique.

IRRFC, UVRFC, VIVL and MBR images complemented the information obtained, as already explained in the previous examples and as shown in Fig. 11.

For completeness of information, some results obtained from MAS.1130 are worthy of mention. This embroidered textile showed a similar result to MAS.911 regarding the brown areas, which were likely to be obtained with a mixture of a plant-based red (probably madder) and tannins. In addition, this textile showed the only examples observed in the textiles investigated of purple obtained as a mixture of a plant-based red (probably madder) and indigo (absorption maxima in the FORS spectra at 510, 540 and 660 nm) and pink obtained from an insect-based dye, most likely lac dye (absorption maxima in the FORS spectra at 525 and 565 nm). Some relevant FORS spectra for this textile and the other textiles discussed above are shown in Fig. 12.

4. Conclusions

Multispectral imaging (MSI) and fibre optic reflectance spectroscopy (FORS) were here applied, with the support of colorimetry and digital microscopy, to a set of reference silk samples dyed with traditional sources of Asian dyes before and after artificial ageing. This protocol, firstly applied to investigate dyes in Late Antique textiles from Egypt [57], was here successfully applied to Asian dyes for the first time, highlighting its versatility and confirming its potential and limitations.

Turmeric, amur-cork tree, cape jasmine, saffron, pagoda tree and yellow safflower were the most light-sensitive among the yellow dyes; sandalwood, sappanwood, red safflower, rosewood and dragon's blood also showed a high degree of fading after ageing among the red dyes. The response exhibited by all the dyes in the various multispectral images (VIS, UVL, IRRFC and UVRFC) was systematically documented and combined with the absorbance features shown in the FORS spectra. The creation of this database highlighted that some of these dyes, such as madder, Indian lac, sappanwood, sandalwood, rosewood, gromwell, safflower, turmeric, saffron, cape jasmine and protoberberine-based yellows (amur-cork tree, Japanese barberry and Chinese goldthread) have a specific combination of responses and/or FORS spectra, which potentially allows for their non-invasive identification. In addition, indigo and tannin-containing dyes can also be identified with this approach, as well as mixtures of these dyes in some cases. By contrast, other yellow dyes gave very similar results to each other and are not clearly distinguishable by these techniques. Other important limitations of this approach emerged. The high concentration of certain dyes on the fibres can quench the emission of luminescence, as in the case of madder; the diameter of the FORS probe (1 mm) does not allow for obtaining clean spectra of very thin areas of colour; evidence for the use of an over-dyeing technique for obtaining mixed colours can be overlooked, as the underlying dye can also be missed by these surface-responsive techniques.

Nevertheless, when applied to thirty-one Chinese textiles from Dunhuang, MSI and FORS succeeded in identifying the main red dyes (safflower, sappanwood, plant-based and insect-based reds – probably madder and Indian lac), highlighting the presence of protoberberine-based yellows, gromwell, indigo and tannins and mapping their distribution. The results were consistent with the current knowledge of the use of dyes in ancient central China, but the methods used here provide a fast and easy-to-interpret way of testing a high number of textiles, providing a holistic view of the materials present thank to point analyses and helping to make decisions about display of these precious and fragile objects.

The information obtained non-invasively was finally extremely useful to design a sampling campaign, with the aim to complement the results by molecular analysis using high pressure liquid chromatography mass spectrometry (HPLC-MS), which is the only method to

unequivocally assess the origin of the dyes. Generally, the results obtained by HPLC-MS were in agreement with the ones obtained non-invasively. In addition, most yellow dyes were identified, madder species were hypothesised in some cases and mixtures of dyes were found to be more frequent than what emerged from the non-invasive data. These results and the related creation of a database of mass spectra for Asian dyes are presented in a separate article.

Acknowledgements

The authors would like to thank the Getty Conservation Institute (Los Angeles, USA) for providing three of the reference samples. Dr Nicole Reifarth (University of Trier) is thanked for her help in the dyeing process of the reference textiles. Monique Pullan (Head of Organics, Conservation Department, British Museum) and Yu-Ping Luk (Curator, Asia Department, British Museum) are thanked for providing access to the archaeological textiles and for their support in the selection and handling of the textiles. As an Andrew W. Mellon Postdoctoral Research Fellow, Diego Tamburini would like to thank the Andrew W. Mellon foundation.

Appendix A. Supplementary data

Supplementary data to this article can be found online at https://doi.org/10.1016/j.dyepig.2018.10.054.

References

[1] Feng Z. Textiles from Dunhuang in UK collections. Shanghai: Donghua University Press; 2007.
[2] Stein A. Ruins of desert cathay: personal narrative of explorations in central Asia and westernmost China. London: Macmillan & Co. Ltd; 1912.
[3] Conservation of ancient sites on the silk Road. Los Angeles: The Getty Conservation Institute; 1997.
[4] Conservation of ancient sites on the silk Road. Los Angeles: The Getty Conservation Institute; 2010.
[5] The conservation of cave 85 at the mogao grottoes, Dunhuang. Los Angeles: The Getty Conservation Institute; 2013.
[6] Cave temples of mogao at Dunhuang: art and history on the silk Road. Los Angeles: The Getty Conservation Institute; 2015.
[7] Temples of Dunhuang Cave. Buddhist art on China's silk Road. Los Angeles: The Getty Conservation Institute; 2016.
[8] Tamburini D, Cartwright CR, Pullan M, Vickers H. An investigation of the dye palette in Chinese silk embroidery from Dunhuang (Tang dynasty). Archaeol. Anthropol. Sci. 2018https://doi.org/10.1007/s12520-017-0592-4.
[9] Cardon D. Natural dyes. Sources, tradition, technology and science. London: Archetype Publications Ltd.; 2007.
[10] Grzywacz CM, Wouters J, Bomin S, Yuquan F. Conservation of ancient sites on the silk Road - Asian organic colourants: a collaborative research project. In: Agnew N, editor. Proc second international conference on the conservation of grotto sites, mogao grottoes. Dunhuang. China: Getty Conservation Institute; 2004.
[11] Han J, Quye A. Dyes and dyeing in the ming and qing Dynasties in China: preliminary evidence based on primary sources of documented recipes. Textile History; 2018. p. 1–27.
[12] Zhang X, Laursen R, Osipova S. Analysis of dyes in some 19th-century Uzbek suzanis. In: Kirby J, editor. The diversity of dyes in history and archaeology. London: Archetype Publications; 2017. p. 339–48.
[13] Jolly A, Vanden Berghe I, Wouters J. Europe or China? Dyestuff analyses as a tool for attributions. In: Kirby J, editor. The diversity of dyes in history and archaeology. London: Archetype Publications; 2017. p. 6–17.
[14] Han J, Wanrooij J, van Bommel M, Quye A. Characterisation of chemical components for identifying historical Chinese textile dyes by ultra high performance liquid chromatography – photodiode array – electrospray ionisation mass spectrometer. J Chromatogr A 2017;1479:87–96.
[15] Gleba M, Vanden Berghe I, Aldenderfer M. Textile technology in Nepal in the 5th-7th centuries CE: the case of Samdzong. STAR: Sci. Technol. Archaeol. Res. 2016;2(1):25–35.
[16] De Luca E, Poldi G, Redaelli M, Zaffino C, Bruni S. Multi-technique investigation of historical Chinese dyestuffs used in Ningxia carpets. Archaeol. Anthropol. Sci. 2016:1–10.
[17] Chen VJ, Smith GD, Holden A, Paydar N, Kiefer K. Chemical analysis of dyes on an Uzbek ceremonial coat: objective evidence for artifact dating and the chemistry of early synthetic dyes. Dyes Pigments 2016;131:320–32.
[18] Liu J, Mouri C, Laursen R, Zhao F, Zhou Y, Li W. Characterization of dyes in ancient textiles from Yingpan, Xinjiang. J Archaeol Sci 2013;40(12):4444–9.
[19] Wouters J, Grzywacz CM, Claro A. A comparative investigation of hydrolysis methods to analyze natural organic dyes by HPLC-PDA - nine methods, twelve biological sources, ten dye classes, dyed yarns, pigments and paints. Stud Conserv 2011;56(3):231–49.
[20] Rodriguez ES, Rodriguez AA, Garcia MA, Camara RC. Characterization of natural and synthetic dyes employed in the manufacture of Chinese garment pieces by LC-DAD and LC-DAD-QTOF. e-conservation magazine 2011;21:38–55.
[21] Mouri C, Laursen R. Identification and partial characterization of C-glycosylflavone markers in Asian plant dyes using liquid chromatography–tandem mass spectrometry. J Chromatogr A 2011;1218(41):7325–30.
[22] Zhang X, Good I, Laursen R. Characterization of dyestuffs in ancient textiles from Xinjiang. J Archaeol Sci 2008;35(4):1095–103.
[23] Zhang X, Corrigan K, MacLaren B, Leveque M, Laursen R. Characterization of yellow dyes in nineteenth-century Chinese textiles. Stud Conserv 2007;52(3):211–20.
[24] Gibbs PJ, Seddon KR, Brovenko NM, Petrosyan YA, Barnard M. Analysis of ancient dyed Chinese papers by high-performance liquid chromatography. Anal Chem 1997;69(10):1965–9.
[25] Sasaki Y, Koike T, Yano T, Sasaki K. Non-destructive dye analysis for the reconstruction of a 17th-century haori fragment in the tokugawa art museum. In: Kirby J, editor. The diversity of dyes in history and archaeology. London: Archetype Publications; 2017. p. 257–64.
[26] Karpova E, Vasiliev V, Mamatyuk V, Polosmak N, Kundo L. Xiongnu burial complex: a study of ancient textiles from the 22nd Noin-Ula barrow (Mongolia, first century AD). J Archaeol Sci 2016;70:15–22.
[27] Kramell A, Li X, Csuk R, Wagner M, Goslar T, Tarasov PE, et al. Dyes of late Bronze Age textile clothes and accessories from the Yanghai archaeological site, Turfan, China: determination of the fibers, color analysis and dating. Quat Int 2014;348:214–23.
[28] Laursen R, Mouri C, Feng Z, Bo L, Jian L. Section III - dyes in ancient Chinese and Japanese textiles. In: Dusenbury MM, editor. Color in ancient and medieval East Asia. New Haven and London: Spencer Museum of Art, University of Kansas, Yale University Press; 2015. p. 81–113.
[29] Padfield T, Landi S. The light-fastness of the natural dyes. Stud Conserv 1966;11(4):181–96.
[30] Saunders D, Kirby J. Light-induced colour changes in red and yellow lake pigments. Natl Gallery Tech Bull 1994;15:79–97.
[31] Kohara N, Sano C, Ikuno H, Magoshi Y, Becker MA, Yatagai M, et al. Degradation and color fading of cotton fabrics dyed with natural dyes and mordant. Historic textiles, papers, and polymers in museums. American Chemical Society; 2000. p. 74–85.
[32] Troalen LG, Röhrs S, Calligaro T, Pacheco C, Kunz S, del Hoyo-Meléndez JM, et al. A multi-analytical approach towards the investigation of Subarctic Athapaskan colouring of quillwork and its sensitivity to photo-degradation. Microchem J 2016;126:83–91.
[33] Ye Y, Salmon LG, Cass GR. The ozone fading of traditional Chinese plant dyes. J Am Inst Conserv 2000;39(2):245–57.
[34] Wouters J, Grzywacz CM, Claro A. Markers for identification of faded safflower (Carthamus tinctorius L.) colorants by HPLC-PDA-MS - ancient fibres, pigments, paints and cosmetics derived from Antique recipes. Stud Conserv 2010;55(3):186–203.
[35] Witkoś K, Lech K, Jarosz M. Identification of degradation products of indigoids by tandem mass spectrometry. J Mass Spectrom 2015;50(11):1245–51.
[36] Manhita A, Santos V, Vargas H, Candeias A, Ferreira T, Dias CB. Ageing of brazilwood dye in wool – a chromatographic and spectrometric study. J Cult Herit 2013;14(6):471–9.
[37] Laursen R, Mouri C. Decomposition and analysis of carthamin in safflower-dyed textiles. e-Preservation Sci 2013;10:35–7.
[38] Zhang X, Cardon D, Cabrera JL, Laursen R. The role of glycosides in the light-stabilization of 3-hydroxyflavone (flavonol) dyes as revealed by HPLC. Microchimica Acta 2010;169(3):327–34.
[39] Degano I, Ribechini E, Modugno F, Colombini MP. Analytical methods for the characterization of organic dyes in artworks and in historical textiles. Appl Spectrosc Rev 2009;44(5):363–410.
[40] Pauk V, Barták P, Lemr K. Characterization of natural organic colorants in historical and art objects by high-performance liquid chromatography. J Separ Sci 2014;37(23):3393–410.
[41] Petroviciu I, Albu F, Medvedovici A. LC/MS and LC/MS/MS based protocol for identification of dyes in historic textiles. Microchem J 2010;95(2):247–54.
[42] Rosenberg E. Characterisation of historical organic dyestuffs by liquid chromatography–mass spectrometry. Anal Bioanal Chem 2008;391(1):33–57.
[43] Lee J, Kang M, Lee K-B, Lee Y. Characterization of natural dyes and traditional Korean silk fabric by surface analytical techniques. Materials 2013;6(5):2007.
[44] Nakamura R, Tanaka Y, Ogata A, Naruse M. Dye analysis of shosoin textiles using Excitation−Emission matrix fluorescence and Ultraviolet−Visible reflectance spectroscopic techniques. Anal Chem 2009;81(14):5691–8.
[45] Sasaki Y, Sasaki K. Dye analysis of a 17th-century historic Japanese textile: a non-destructive approach. In: Kirby J, editor. The diversity of dyes in history and archaeology. London: Archetype Publications; 2017. p. 265–77.
[46] Mounier A, Le Bourdon G, Aupetit C, Lazare S, Biron C, Pérez-Arantegui J, et al. Red and blue colours on 18th–19th century Japanese woodblock prints: in situ analyses by spectrofluorimetry and complementary non-invasive spectroscopic methods. Microchem J 2018;140:129–41.
[47] Derrick M, Newman R, Wright J. Characterization of yellow and red natural organic colorants on Japanese woodblock prints by EEM fluorescence spectroscopy. J Am Inst Conserv 2017;56(3–4):171–93.
[48] de Ferri L, Tripodi R, Martignon A, Ferrari ES, Lagrutta-Diaz AC, Vallotto D, et al. Non-invasive study of natural dyes on historical textiles from the collection of

Michelangelo Guggenheim. Spectrochim Acta Mol Biomol Spectrosc 2018;204:548–67.
[49] Aceto M, Agostino A, Fenoglio G, Idone A, Gulmini M, Picollo M, et al. Characterisation of colourants on illuminated manuscripts by portable fibre optic UV-visible-NIR reflectance spectrophotometry. Anal. Meth. 2014;6(5):1488–500.
[50] Gulmini M, Idone A, Diana E, Gastaldi D, Vaudan D, Aceto M. Identification of dyestuffs in historical textiles: strong and weak points of a non-invasive approach. Dyes Pigments 2013;98(1):136–45.
[51] Gulmini M, Idone A, Davit P, Moi M, Carrillo M, Ricci C, et al. The “Coptic” textiles of the “Museo Egizio” in Torino (Italy): a focus on dyes through a multi-technique approach. Archaeol. Anthropol. Sci. 2016:1–13.
[52] Clementi C, Doherty B, Gentili PL, Miliani C, Romani A, Brunetti BG, et al. Vibrational and electronic properties of painting lakes. Appl Phys A 2008;92(1):25–33.
[53] Dyer J, Sotiropoulou S. A technical step forward in the integration of visible-induced luminescence imaging methods for the study of ancient polychromy. Heritage Sci. 2017;5(1):24.
[54] Verri G. Pezzati L, Salimbeni R, editors. The application of visible-induced luminescence imaging to the examination of museum objects. 1 ed.Munich, Germany: SPIE; 2009. p. 739105–12.
[55] Verri G, Opper T, Devièse T. The ‘Treu Head’: a case study in Roman sculptural polychromy. British Museum Tech. Res. Bull. 2010;4:39–54.
[56] Dyer J, O'Connell ER, Simpson A. Polychromy in Roman Egypt: a study of a limestone sculpture of the Egyptian god Horus. British Museum Tech. Res. Bull. 2014;8:93–103.
[57] Dyer J, Tamburini D, O'Connell ER, Harrison A. A multispectral imaging approach integrated into the study of Late Antique textiles from Egypt. PloS One 2018;13(10):e0204699.
[58] Dyer J, Verri G, Cupitt J. Multispectral imaging in reflectance and photo-induced luminescence modes: a user manual. 2013.
[59] Kirby J, van Bommel M, Verhecken A. Natural colorants for dyeing and lake pigments. London: Archtype Publications; 2014.
[60] Collins S, Davidson RS, Hilchenbach MEC, Lewis DM. The natural fluorescence of wool. Dyes Pigments 1994;24(2):151–69.
[61] Kirby J, Spring M, Higgitt C. The technology of red lake pigment manufacture: study of the dyestuff substrate. Natl Gallery Tech Bull 2005;26:71–87.
[62] Clementi C, Basconi G, Pellegrino R, Romani A. Carthamus tinctorius L.: a photophysical study of the main coloured species for artwork diagnostic purposes. Dyes Pigments 2014;103:127–37.
[63] Diaz MS, Freile ML, Gutierrez MI. Solvent effect on the UV/Vis absorption and fluorescence spectroscopic properties of berberine. Photochem Photobiol Sci 2009;8(7):970–4.
[64] Erez Y, Simkovitch R, Shomer S, Gepshtein R, Huppert D. Effect of acid on the ultraviolet–visible absorption and emission properties of curcumin. J Phys Chem 2014;118(5):872–84.